



Evaluation of activated carbon for remediating benzene contamination: Adsorption and oxidative regeneration

Chenju Liang*, Yan-Jyun Chen

Department of Environmental Engineering, National Chung Hsing University, 250 Kuo-kuang Road, Taichung 402, Taiwan

ARTICLE INFO

Article history:

Received 9 August 2009

Received in revised form 29 April 2010

Accepted 16 June 2010

Available online 23 June 2010

Keywords:

Persulfate

Permeable reactive barrier

In situ chemical oxidation

Pyrite

Groundwater remediation

ABSTRACT

This study investigated the potential usage of activated carbon (AC) as a permeable reactive barrier material for the adsorption of benzene contaminant. Sodium persulfate (SPS) or pyrite (FeS_2) activated SPS oxidation was used for the regeneration of spent AC. Results indicate that persulfate oxidation of AC caused a loss of electrons and a reduction in adsorptive capacity due to the formation of acidic functional groups on the AC. Concerning the reactants that can be used for oxidation of the benzene contaminants, SPS/ FeS_2 /AC, as oppose to SPS/AC, can achieve benzene destruction in both the aqueous and the sorbed phases. Furthermore, regeneration of benzene spent AC by SPS or SPS/ FeS_2 revealed that SPS oxidation resulted primarily in desorption of benzene over direct oxidation of AC sorbed benzene. In contrast, the SPS/ FeS_2 system achieved complete oxidation of desorbed benzene in the aqueous phase while also oxidizing sorbed benzene. Results of re-adsorption show that oxidative regeneration recovered around 70% of the AC adsorption sites and the remaining capacity was mostly occupied by the residual benzene on the AC. This study demonstrates that SPS or FeS_2 activated SPS oxidation is an effective alternative method for the regeneration of spent AC.

© 2010 Elsevier B.V. All rights reserved.

1. Introduction

Benzene is classified as a toxic, carcinogenic and mutagenic compound [1]. In the United States, gasoline is generally composed of 2% benzene by volume but the concentration of benzene in gasoline may be up to 5% in other countries [2]. It should be noted that benzene, with a water solubility of 1780 mg/L, is more water soluble than other major gasoline components. Therefore, if accidental leakage occurs from an underground gasoline storage tank, benzene would pose a serious threat to the groundwater system and the public who drink the benzene contaminated groundwater for a long time would be potentially at risk of developing cancer risk. The United States Environmental Protection Agency (EPA) and Taiwan EPA have both set the maximum contaminant level for benzene in drinking water and groundwater at 0.005 mg/L.

Adsorption processes have been widely applied for the treatment of drinking water [3] and industrial wastewater [4]. Furthermore, adsorption with activated carbon (AC) is one of the reaction mechanisms applied in the permeable reactive barrier (PRB) technique for groundwater remediation. The adsorptive capacity of AC in the aqueous phase mainly depends on three factors [5–7]: (1) the characteristics of the AC such as the sur-

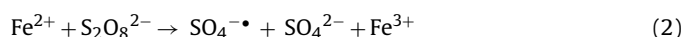
face chemistry (e.g., surface functional groups and ash content) and texture (e.g., surface area and pore size distributions), (2) the characteristics of the adsorbate (e.g., pK_a , functional groups present, polarity, and molecular weight and size) and (3) the solution conditions (e.g., pH, temperature, adsorbate concentration, the presence of competitive compounds and polarity of solvent). Furthermore, these factors can be classified into three types of interactions: adsorbate–AC, adsorbate–solution and AC–solution [8]. Due to attraction occurring between the π orbital on the carbon basal planes and the electronic density in the benzene aromatic rings (π – π interactions) [6,9], AC adsorption of benzene (i.e., adsorbate–AC interaction) is mainly governed by nonspecific dispersion physical adsorption forces. Adsorbate–solution interaction is related to the chemical compatibility of the adsorbate with the solution used (e.g., adsorbate solubility in water). Therefore, a contaminant with more hydrophobic characteristics (e.g., benzene) can induce a greater driving force for adsorption in the aqueous phase. The AC–solution interaction is governed by the surface polarity and functional groups of the carbon surfaces. The polar sites present growing centers of water clusters in the micropores that hinder hydrophobic adsorbate adsorption by AC. Owing to the functional groups of AC classified as acidic (oxygen-containing) and basic (nitrogen-containing), the surface of the AC exhibits different polarities [8].

The selection criteria for the reactive media in PRB are based on reactivity, stability, availability, cost, hydraulic performance, envi-

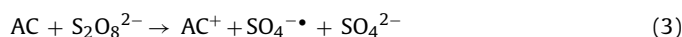
* Corresponding author. Tel.: +886 4 22856610; fax: +886 4 22856610.
E-mail address: cliang@dragon.nchu.edu.tw (C. Liang).

ronmental compatibility and safety [10]. Activated carbon used as a PRB reactive material for benzene removal fits well with the above criteria well. However, hydraulic performance of subsurface is largely dependent on the hydraulic conditions of the site and other factors such as temperature and the composition of the groundwater. However, when certain reactive materials are used to treat contaminants that have been present in the subsurface for decades, the long-term efficiency of PRB is a matter of great concern [11]. Therefore, there is a requirement for a feasible in situ recycling method capable of extending the lifecycle of a PRB.

Persulfate ($S_2O_8^{2-}$) is the latest oxidant to be used for in situ chemical oxidation (ISCO) of soil and groundwater contaminants. It is a highly reactive oxidant ($E^0 = 2.01$ V), yet is more stable and persistent in the subsurface than hydrogen peroxide, another ISCO oxidant. ISCO using persulfate and activated persulfate has emerged as a viable remediation technology for the treatment of subsurface contaminants. Persulfate activation, an advanced oxidation process (AOP), to generate sulfate radicals ($SO_4^{\bullet-}$) has been demonstrated as an effective means of destroying aromatic organics such as benzene, toluene, ethyl benzene and xylene [12–14]. Persulfate activation using heat (e.g., 30–99 °C) and the presence of transitional metals (e.g., Fe^{2+}) can generate $SO_4^{\bullet-}$ in accordance with Eqs. (1) and (2) [15], respectively.

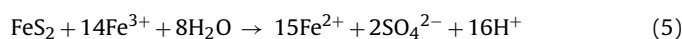
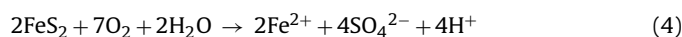


The AC surface is partly comprised of residual electrons and ion-exchange functional groups [16], which can induce electron transfer activation. The hydrogen peroxide/AC heterogeneous activation mechanism has been shown to effectively destroy organics [17,18] and regenerate exhausted AC [19]. In a similar theory, put forward by Kimura and Miyamoto [20], it is stated that AC may also activate persulfate via electron transfer and produce $SO_4^{\bullet-}$ in accordance with the following equation:



where AC^+ : the oxidizing cation-radical activated carbon.

Furthermore, pyrite (FeS_2), a natural Fe^{2+} -bearing sulfide mineral, can be oxidized using O_2 (Eq. (4)) and Fe^{3+} (Eq. (5)) to gradually release Fe^{2+} [21] and therefore be a possible source of Fe^{2+} for persulfate activation in accordance with Eq. (2). The mixture of pyrite with PRB reactive materials (e.g., zero valent iron) has been used to serve as an on-site method for producing sulfuric acid during PRB operations and to moderate the pH of the reactive bed, thereby decreasing the amount of precipitates formed in PRB [22].



Therefore, when combing the activated persulfate AOP and AC or AC/ FeS_2 filled PRB, the $SO_4^{\bullet-}$ generated by AC or FeS_2 induced persulfate activation may be of benefit as it can provide “on-site chemical oxidative regeneration” for in situ destruction of AC sorbed contaminants, recycling of spent AC, and maintenance of the longevity and effectiveness of PRB. This will lead to a reduction in the cost of retrieving the reactive materials from the existing PRB.

The objectives of this study were to investigate the potential usage of AC as a reactive material in the presence or absence of pyrite to accumulate contaminants within PRB, in conjunction with the use of persulfate for recycling reactive materials. This paper addresses three issues: (1) the impact of persulfate oxidation on the properties of AC for benzene adsorption; (2) persulfate oxidation of benzene in the presence of AC or AC/pyrite; (3) the evaluation of recycling benzene spent AC with persulfate or pyrite activated persulfate.

2. Materials and methods

2.1. Chemicals

Water used was purified using a Millipore reverse osmosis (RO) purification system. Sodium bicarbonate ($NaHCO_3$, min. 99.7%, Riedel-deHaën) and potassium iodide (KI, min. 99.5%, UNION Taiwan) were used for persulfate analysis. Carbon disulfide (CS_2 , 99.9%, Riedel-deHaën) was used for benzene extraction. Sulfuric acid (H_2SO_4 , >99.8%, Fluka), nitric acid (HNO_3 , >65%, Fluka), sodium nitrate ($NaNO_3$, min. 99.0%, Riedel-deHaën) and sodium hydroxide ($NaOH$, min. 99.0%, Riedel-deHaën) were used for determining the point of zero charge (pH_{pzc}). Methanol (CH_3OH , 99.9%, ECHO) was used for preparing a series of benzene standard solutions. Sodium persulfate ($Na_2S_2O_8$, min. 99.0%) was purchased from Merck; benzene (C_6H_6 , min. 99.7%) was purchased from Riedel-deHaën; pyrite (FeS_2 , 99.9% powder) was purchased from Alfa Aesar. A commercial activated carbon Calgon Filtrasorb 300 (F300) (a bituminous-coal-based carbon) was obtained from Calgon Carbon Corporation. All of the AC used (particles sieved: 2.0–1.2 mm) in this experiment was prepared by acid washing with 5% HCl for 24 h to remove impurities present in the carbon and rinsed with RO water until the pH of the solution was stable [23]. The AC was then dried at 105 °C for 24 h prior to storage in a desiccator.

2.2. Experimental setup

2.2.1. Degradation of persulfate on the activated carbon

The experiments were performed to consider two aspects: the effects of AC doses (0, 2, 5 g/L) under a fixed SPS concentration of 2 g/L and the effects of sodium persulfate (SPS) concentrations (1, 2, 5 g/L) under a fixed AC dose of 5 g/L. All experiments were conducted in 1 L volumetric flasks that were capped and stirred at 20 °C in a temperature-controlled chamber (KANSIN low-temp incubator, LT1603). For all tests in this study, the pH of the RO water was initially adjusted to pH 3 using 0.05N sulfuric acid before the addition of the reactants. After the reactions had finished, the OAC-1 and OAC-5 were washed with RO water several times until the pH of the solution was stable. The OAC-1 and OAC-5 were then dried in an oven under 50 °C for further preservation in a desiccator and subsequent analysis of surface properties. Note that the notations OAC-1 and OAC-5 represent the products of the AC that were oxidized with 1 and 5 g/L of SPS, respectively.

2.2.2. Adsorption kinetics and isotherms

For the adsorption kinetic experiments, a benzene solution (60 mg/L, pH 3) was prepared by adding the required amount of pure benzene and stirring for 12 h in a 1.36 L heavy-walled plain pressure reaction flask (IWAKI 7740 glass) with no head space. The flask was then placed in a temperature-controlled chamber at 20 °C and the top of the flask was covered and clamp-sealed with a flat Teflon reaction head equipped with Teflon-lined septum ports. For determining the kinetics of the benzene adsorption process, various experimental conditions (AC (0.5–5 g/L), OAC-5 (1.5 g/L) and AC (5 g/L)/ FeS_2 (0.5 g/L)) were used separately. At each sampling time, 1 mL of solution was withdrawn through a septum port using a 1-mL gas-tight syringe (SGE gas-tight syringe, fitted with push-button luer-lock valve) and filtered using a 0.2 μ m PTFE filter placed within a stainless syringe holder (ADVANTEC, KS-13).

Equilibrium isotherm experiments were conducted using the bottle-point method. The benzene solution (60 mg/L, pH 3) was prepared in a 2.3 L borosilicate reservoir (Schott Puran) equipped with a Teflon stopper and valved bottom outlet. The solution was then added to a series of 120 mL amber crimped-top reaction bottles with no head space, in which different AC, OAC-1 or OAC-5 doses in the range of 0.1–5 g/L were initially added. When adsorp-

tion reached equilibrium (magnetically stirred for 24 h, a period based on results from the adsorption kinetic experiments), sample solutions were taken using a gas-tight syringe and filtered for benzene analysis.

2.2.3. Oxidation experiments

Oxidation systems including $\text{AC}/\text{S}_2\text{O}_8^{2-}$, $\text{FeS}_2/\text{S}_2\text{O}_8^{2-}$ and $\text{AC}/\text{FeS}_2/\text{S}_2\text{O}_8^{2-}$ were conducted for treating benzene (60 mg/L, pH 3) in accordance with the procedure of the adsorption kinetic experiments described in Section 2.2.2. The AC and FeS_2 doses were 5 and 0.5 g/L, respectively, and two concentration levels (2 and 5 g/L) were used for SPS. In order to record the relative quantities of benzene which were sorbed, oxidized and remained in the aqueous phase, the aqueous benzene concentration was analyzed and the AC sorbed benzene was extracted using carbon disulfide for analysis. Note that in all 2 g/L SPS experiments, the AC was extracted until the SPS was almost exhausted, i.e., after 5 h (this period was based on experimental results). Additionally, for the 5 g/L SPS experiments, two separate runs were conducted, in which one where the AC was extracted after 5 h for comparison and in the other where extraction was carried out after 24 h. The AC extraction procedure used is as follows: the solution was filtered (Advantec 0.45 μm cellulose ester filter), approximate 0.1 g residual AC was weighed into each 5 mL brown bottle (6 replicates), 3 mL carbon disulfide was added, and then the bottles were shaken for 5 min at 1400 rpm on a vortex shaker. AC extraction was also performed for the AC adsorption only in the adsorption kinetic experiment to ensure the recovery of benzene during the extraction processes. Control tests in the absence of persulfate, AC or FeS_2 were carried out in parallel.

2.2.4. Regeneration of benzene spent AC

Adsorption experiments in the absence and presence of FeS_2 (0.5 and 1.0 g/L) were conducted in accordance with the procedure described in Section 2.2.2. When equilibrium was reached, SPS (2 g/L) was added into each reactor. After the SPS was exhausted, the solution was carefully decanted and filtered to allow the majority of the AC to remain in the reactor. Following this, the AC that remained on the filter was oven-dried at 105 °C and measured to determine the loss of AC. Thereafter, fresh benzene solution was added for re-adsorption experiments. Aqueous benzene concentrations were measured throughout all processes. A separate run was also conducted and then the AC was sacrificed for analysis of the sorbed benzene concentration.

2.3. Analytical methods

The point of zero charge (pH_{pzc}) for the AC surfaces was measured by mass titration as described by Noh and Schwarz [24]. BET surface area and pore volumes were determined by N_2 adsorption at 77 K (Micromeritics ASAP 2020, high surface area and porosimetry analyzer). The aqueous benzene concentration was measured using a high performance liquid chromatography/UV (Agilent 1100) equipped with a reversed-phase ZORBAX Eclipse XDB-C18 (4.6 mm \times 150 mm \times 5 mm) column (mobile phase using acetonitrile/water (70/30, v/v) with a flow rate at 1.00 mL/min and the effluent monitored at 254 nm). The AC sorbed benzene was extracted using carbon disulfide and the extract was analyzed using gas chromatography (Agilent 6890N)/flame ionization detector/autosampler (Agilent 7683B) and an Agilent HP-5 fused silica capillary column (30 mm \times 0.32 mm \times 0.25 μm) (nitrogen as the carrier gas at a flow rate of 15 mL/min and temperatures for column, injector, and detector: 45 (isothermal), 220, and 250 °C, respectively). Persulfate was monitored using the spectrophotometric method ($\lambda = 400 \text{ nm}$) [25]. pH was monitored using a ROSS pH combination electrode and a pH/Ion meter (Thermo Orion 720A+).

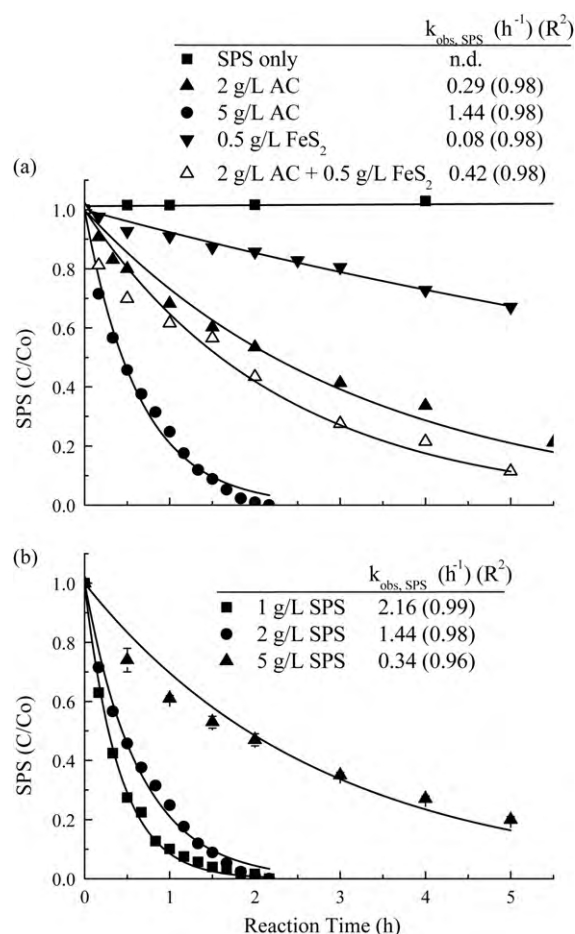


Fig. 1. Sodium persulfate degradation in the presence of AC and/or FeS_2 under (a) a fixed persulfate concentration ($[\text{SPS}]_0 = 2 \text{ g/L}$); (b) a fixed AC dosage ($[\text{AC}]_0 = 5 \text{ g/L}$). n.d. = not determined.

3. Results and discussion

3.1. Impact of persulfate oxidation on AC

3.1.1. Decomposition kinetics of persulfate

The results of persulfate decomposition in the presence of AC under a fixed persulfate concentration and a fixed AC dosage are presented in Fig. 1a and b, respectively. It can be seen that the decomposition of persulfate in this study fits a pseudo-first-order kinetic model well, with correlation coefficients of >0.96 calculated. It should be noted that the velocity of a reaction between persulfate and AC, when the AC is present at a concentration greatly in excess of that of the persulfate and assuming that the concentrations do not change throughout the course of the reaction, is determined only by the concentration of the persulfate. This is therefore an example of a pseudo-monomolecular reaction, because the velocity of the reaction is determined by the concentration of only one of the two reactants (i.e., persulfate) and yet still follows first-order kinetics. Furthermore the observed rate constants were found to decline when persulfate concentration increased and the AC dosage was lowered (data presented in inset tables in Fig. 1). These were analogous to the hydrogen peroxide decomposition kinetics in the presence of AC reported in the literature [17,26]. Since AC surface contact is the rate-controlling step for the overall persulfate or peroxide decomposition reaction [17], the surface characteristics of AC play an important role in influencing the interaction between persulfate and AC.

Table 1

The physical and chemical characteristics of activated carbon.

AC type	BET surface area (m ² /g)	Pore volume (cm ³ /g)	Pore area (cm ² /g)	pH _{pzc}	Acidity (mmol/g)	Basicity (mmol/g)
AC	722.88	0.087	112.7	7.8	0.707	0.548
OAC-1	668.70	0.083	108.5	2.8	1.357	0.281
OAC-5	677.13	0.075	103.0	3.6	2.599	0.013

As can be seen in Table 1, the specific surface area, pore volume, pore area, pH_{pzc} and basicity of AC decreased after persulfate oxidation with the exception that acidity increased significantly when persulfate concentration increased. Due to the fact that persulfate and sulfate radicals are strong oxidizing reagents, they would oxidize carbon atoms and cause the AC surface to lose its electrons (i.e., π electrons). Consequently, the AC surface would become positively charged and this would lead to a decrease in pH_{pzc} [27–29]. Note that the results for mass titration to determine pH_{pzc} are presented in Fig. S11 (Supporting Information). Therefore, surface interaction phenomena involving persulfate over the AC would be associated with the AC surface oxygen functional groups and the presence of delocalized π electrons on the oxygen-free Lewis basic sites that are situated on the basal planes of AC [6]. Thus, it can be suggested that the interaction between persulfate and AC may involve the exchange of an oxonium-hydroxyl group (e.g., AC surface C–OH₂⁺OH[−]) with persulfate anions [20,30] and this may decrease the total surface area of the AC [31]. Moreover, Liang et al. [32], using Fourier transform infrared spectroscopy analysis, demonstrated that the acidic functional groups on the persulfate oxidized AC are possibly the C–O–C asymmetric stretching modes of the ether or ester and the ether–oxygen (ascribed to C–O single bonds).

Additionally, it can be seen that pyrite caused slow persulfate decomposition (Fig. 1a). The surface of pyrite surface contains unshared pairs of electrons and it is evident that the release of Fe²⁺ from the pyrite (in accordance with Eqs. (4) and (5)) induced slow persulfate decomposition. Persulfate decomposition rates in the presence of both pyrite and AC were slightly higher than those in the presence of AC only (i.e., increased from 0.29 to 0.42 h^{−1}). As a result of this side effect, pyrite activated persulfate may assist in destroying AC sorbed contaminants. Further evaluation of this will be presented in the following sections.

3.1.2. Benzene adsorption kinetics and isotherm

Fig. 2 shows the adsorption kinetics for benzene reacting with AC, OAC-5 and AC/FeS₂. It can be seen that the time required for reaching adsorption equilibrium for different AC doses was less than 10 h and that the adsorption kinetics and capacity of the AC were not influenced by the presence of pyrite. Also, a control test demonstrated that little benzene adsorption by pyrite occurred (0.5 g/L) (discussed in Section 3.2). In order to examine the mechanisms of the adsorption process, three simplified kinetic models, i.e., pseudo-first-order equation (Eq. (6)), pseudo-second-order equation (Eq. (7)) and intra-particle diffusion (Eq. (8)) [33], were employed and the results can be seen in Fig. S12 and Table S11 (Supporting Information).

$$\ln(q_e - q_t) = \ln q_e - k_1 t \quad (6)$$

$$\frac{t}{q_t} = \frac{1}{k_2 q_e^2} + \left(\frac{1}{q_e}\right) t \quad (7)$$

$$q_t = k_{df} t^{0.5} + C \quad (8)$$

where q_e and q_t are the amounts of benzene adsorbed (mg/g) at equilibrium and at time t (h), respectively; k_1 and k_2 are rate constants of pseudo-first-order (h^{−1}) and pseudo-second-order sorption (g/(h mg)); k_{df} is the intra-particle diffusion rate constant

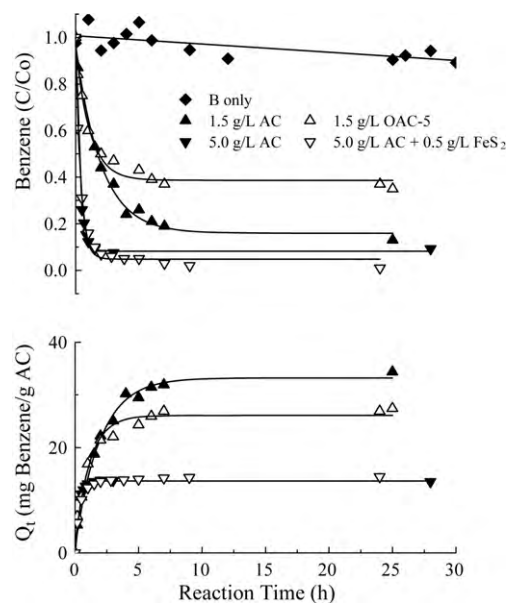


Fig. 2. Benzene adsorption kinetic profiles. Note: B: benzene.

(mg/(g h^{−0.5})); C is the intercept that represents the value of the thickness of the boundary layer.

The results show that both pseudo-first- and pseudo-second-order kinetic models well fit data ($R^2 > 0.93$) and can be used to describe benzene adsorption kinetic behavior while pseudo-second-order kinetic model revealed an even higher correlation (i.e., $R^2 > 0.98$). The decomposition of persulfate on AC may be ascribed to the chemical exchange of an oxonium-hydroxyl group with persulfate anions to form acidic functional groups (e.g., AC surface C–OH₂⁺HSO₄[−]) [30,31]. Therefore, functional groups present on the AC may play a role in electrostatic interactions with persulfate anions. It should be noted that the term pseudo-second-order kinetic behavior more accurately describes sorption behavior which involves valence force through the sharing of electrons between an adsorbent and an adsorbate [34,35]. Furthermore, the benzene adsorption equilibrium capacities were analyzed using two isotherm models (Freundlich and Langmuir models, as shown in Eqs. (9) and (10), respectively), to assess their efficiencies [36].

$$Q_e = K_f C_e^{1/n} \quad (9)$$

$$Q_e = q_m \frac{b C_e}{1 + b C_e} \quad (10)$$

where K_f and n are Freundlich isotherm parameters, representing the unit capacity factor ((mg g^{−1})(L mg^{−1})^{1/n}) and intensity of adsorption (dimensionless), respectively; q_m and b are Langmuir isotherm parameters, representing the maximum adsorption monolayer capacity (mg-benzene/g-AC) and affinity constant (L g^{−1}), respectively. Fig. 3a and b illustrates the AC isotherm adsorption of benzene and correlations between the isotherm parameters and acidity on the AC surface are presented in Fig. 3c and d. The adsorptive capacity of the OAC and the isotherm parameters decreased when AC surface acidities increased as a result of persulfate oxidation of the AC. Also, as indicated in the previous

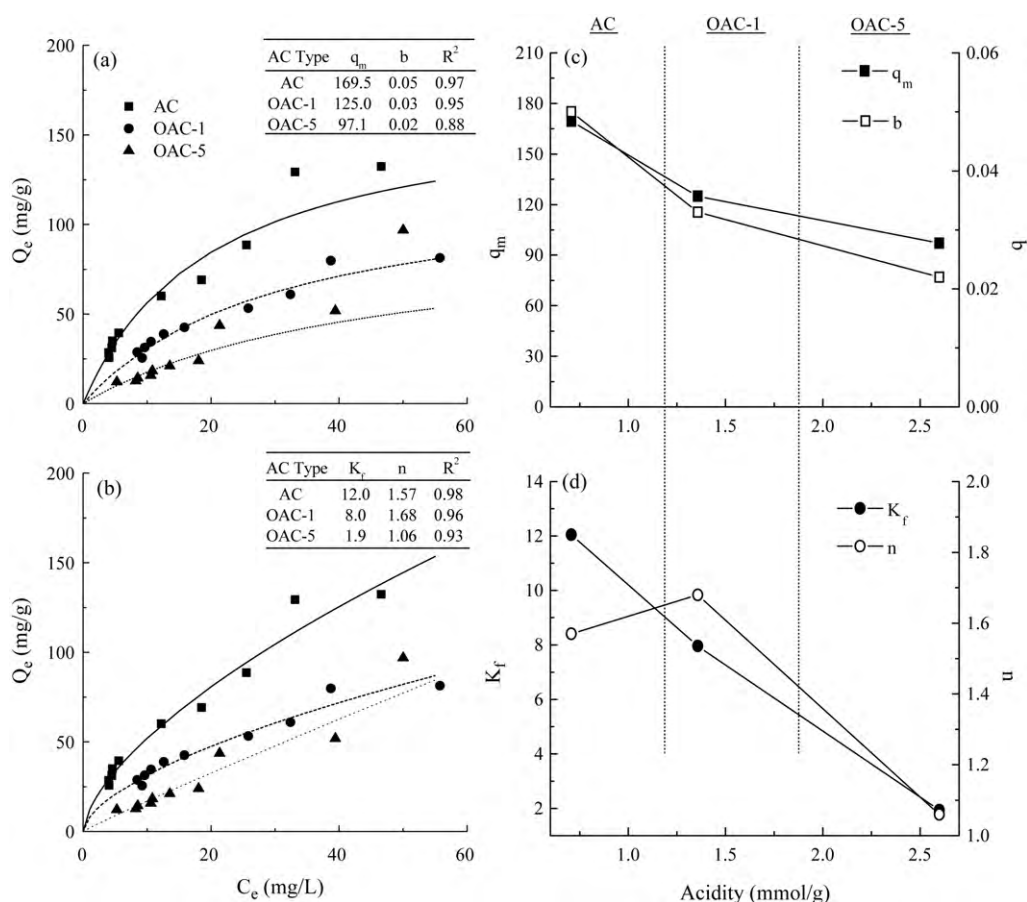


Fig. 3. Isotherm plots of benzene onto AC and OAC-1, -5: (a) Langmuir and (b) Freundlich desorption isotherm a function of acidity; (c) Langmuir: q_m , b and (d) Freundlich: K_f , n .

section, the higher initial persulfate concentration resulted in a greater degree of acidity. Since benzene is in the molecular form in solution, the adsorption mechanism occurs mainly by dispersive attraction between the π orbital on the carbon basal planes and the electronic density in the benzene aromatic rings (π - π interactions) [6,9]. Persulfate oxidation of the AC surface triggered losses of electrons from the AC and produced acidic functional groups, which lead to a weakening of the AC dispersive interaction with benzene and the formation of water clusters [37,38]. As a result, some AC pores became blocked and inaccessible for benzene adsorption and hence resulted in decreases in adsorptive capacity.

3.2. Persulfate oxidation of benzene in the presence of AC or AC/pyrite

Fig. 4 shows the influence of the simultaneous presence of persulfate and AC or persulfate/ FeS_2 and AC on benzene adsorption and degradation. The presence of persulfate appeared to reduce benzene adsorption (see Fig. 4a). Moreover, the presence of benzene slowed down the decomposition of persulfate by AC (e.g., $k_{\text{obs,SPS}} = 1.44 \text{ h}^{-1}$ in Fig. 1b vs. $k_{\text{obs,SPS}} = 0.68 \text{ h}^{-1}$ in Fig. 4c). This phenomenon was similar to that observed by Lucking et al. [26] who used AC for H_2O_2 activation and 4-chlorophenol adsorption. Lucking et al. [26] reported that the adsorption of 4-chlorophenol delayed the peroxide decomposition and that the peroxide caused a reduction in the adsorptive capacity of the AC. Adsorption of benzene-occupied active sites occurred on the AC which then became unavailable for activating persulfate and resulted in a slower rate of persulfate decomposition. Additionally, the analysis of benzene distribution in the system demonstrates that the

AC sorbed benzene decreased from 52% to 37% when the SPS doses increased from 2 to 5 g/L (see Fig. 4d). Furthermore, the AC sorbed benzene remained nearly unchanged (about 3% difference) when the reaction time was extended from 5 to 24 h. However, when a reaction time of 24 h was used, the aqueous benzene was further degraded according to Eq. (3) and persulfate was completely decomposed. It can be deduced that a quantity of the AC sorbed benzene was unreactive or unreachable by persulfate. When H_2O_2 and AC were combined to oxidize various hydrophobic compounds, similar observations were reported and depending on the hydrophobicities of the organics [18], some of the sorbed fractions were found to be almost unreactive.

Fig. 4b shows that pyrite activated persulfate offers a more effective method for destroying benzene when compared to the results obtained from the persulfate oxidation of benzene. The rates of benzene removal were fairly similar in the systems using AC/SPS/ FeS_2 (5/2/0.5) and AC only (see Fig. 4a) (i.e., $k_{\text{obs,benzene}} = 2.21$ and 2.50 h^{-1}). Moreover, the rates achieved in the systems using AC/SPS/ FeS_2 were faster than those in the systems using SPS/ FeS_2 (i.e., $k_{\text{obs,benzene}} = 0.53 \text{ h}^{-1}$, in the absence of AC) (see Fig. 4b) and AC/SPS (i.e., $k_{\text{obs,benzene}} = 1.56 \text{ h}^{-1}$, in the absence of FeS_2) (see Fig. 4a). Hence, these results suggest that the existence of AC in the SPS/ FeS_2 system enhances benzene degradation. The differences in k_{obs} for benzene degradations were due to AC adsorption. Furthermore, the role of pyrite can be demonstrated by comparing the results of the AC/SPS/ FeS_2 system to those of the AC/SPS and AC only systems. No benzene remained in the aqueous phase in the AC/SPS/ FeS_2 system whereas around 10% remained in the system that used only AC adsorption (see Fig. 4d) and 51% vs. 11% of sorbed benzene in the system of AC/SPS = 5/2 vs. AC/SPS/ FeS_2 = 5/2/0.5.

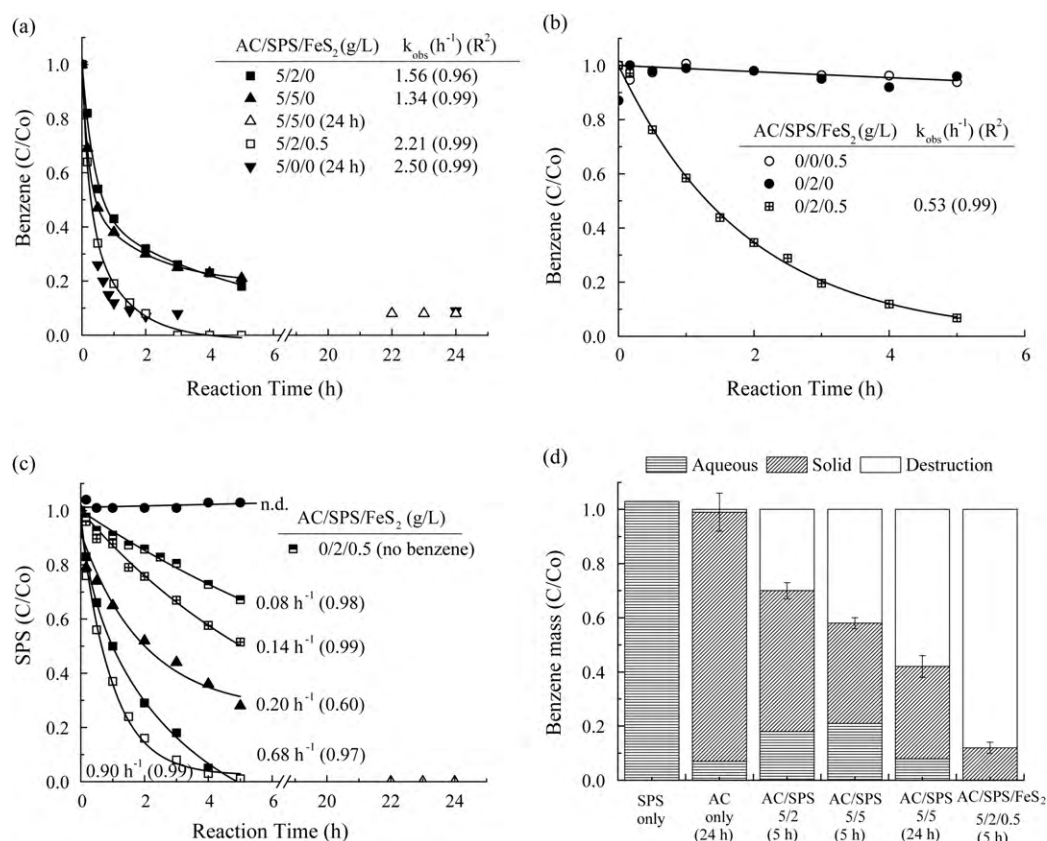
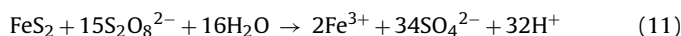
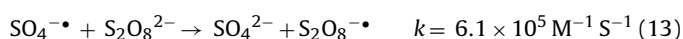
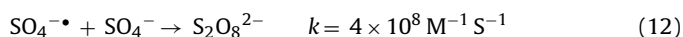


Fig. 4. Oxidation of benzene under various experimental conditions: (a) in the presence of AC and (b) in the absence of AC; (c) persulfate degradations; (d) mass balance among different phases.

Therefore, it can be seen that the addition of pyrite as a source of Fe²⁺ to activate persulfate can aid in achieving complete destruction of benzene in both the aqueous and the sorbed phases. However, it was observed that the presence of benzene in the SPS/FeS₂ system resulted in a faster decomposition rate than that of the system where no benzene was present (i.e., 0.14 vs. 0.08 h⁻¹) (see Fig. 4c). The explanation of this can start from the reaction of persulfate and pyrite as shown in Eq. (11).



Persulfate first reacts with pyrite to produce Fe³⁺ and as a subsequent step, pyrite is then oxidized by Fe³⁺ to generate Fe²⁺ in accordance with Eq. (5). It has been reported that oxidation of pyrite by Fe³⁺ is faster than that achieved by molecular oxygen in an acidic solution, that is Eq. (4) [39]. Since Fe²⁺ is the active species in activating persulfate and a limiting reagent, SO₄^{-•} formed upon persulfate activation in the absence of benzene may be scavenged by SO₄^{-•} and/or persulfate, according to Eqs. (12) and (13) [40]. However, if benzene is present, due to a fast reaction rate constant for reactions between SO₄^{-•} and benzene (i.e., 3 × 10⁹ M⁻¹ S⁻¹ [41]), a significant quantity of SO₄^{-•} would be scavenged by benzene. Therefore, in the presence of benzene, Fe³⁺ would accumulate faster and the pyrite would subsequently be oxidized by Fe³⁺ to release Fe²⁺ for decomposing persulfate. Hence, the observed decomposition rate of persulfate was faster when benzene was present.



3.3. Persulfate regenerating AC with and without pyrite

Fig. 5 shows the results of the regeneration of benzene spent AC by persulfate or persulfate/FeS₂. During the course of regeneration, persulfate oxidation resulted in the presence of benzene in the aqueous phase, implying that desorption of benzene was dominant over direct oxidation of sorbed benzene by AC activated persulfate. On the other hand, no aqueous benzene was detected when pyrite activated persulfate oxidation (i.e., two different pyrite doses) was used, implying that more complete oxidation of aqueous benzene occurred than when using persulfate oxidation alone. Moreover, persulfate decomposition rates increased from 0.67 h⁻¹ (in the presence of AC) to 1.03 h⁻¹ (in the presence of AC and pyrite 0.5 g/L). At the end of the regeneration period (i.e., 5 h) and when pyrite had been used, the residual AC sorbed benzene was found to be less than that remaining after oxidation using persulfate only (e.g., 38% residual by persulfate vs. 33% residual by 0.5 g/L pyrite activated persulfate oxidation) (see Fig. 5c). Nevertheless, some AC sorbed benzene appeared occupation of the adsorption sites or to be un-accessible for oxidation.

The amounts of benzene sorbed after regeneration were 5.35 and 4.55–4.67 mg-benzene/g-AC for persulfate and pyrite activated persulfate oxidation, respectively (data presented in inset table in Fig. 5c). Compared to the initial adsorptive capacity (i.e., 14.73 mg-B/g-AC), the re-adsorptive capacity decreased by around 30% (e.g., (14.73 – 10.72)/14.73 = 27%). This is partially attributable to the residual benzene on the AC. However, the total adsorptive capacity slightly increased by around 4–10%. When comparing the results of re-adsorptive capacity for AC regenerated from spent AC with those for OAC (pre-oxidized) (see discussion in Section 3.1.2), it can be seen that persulfate oxidation of benzene spent AC appeared to less adversely influence the adsorptive capacity of the AC. This is pos-

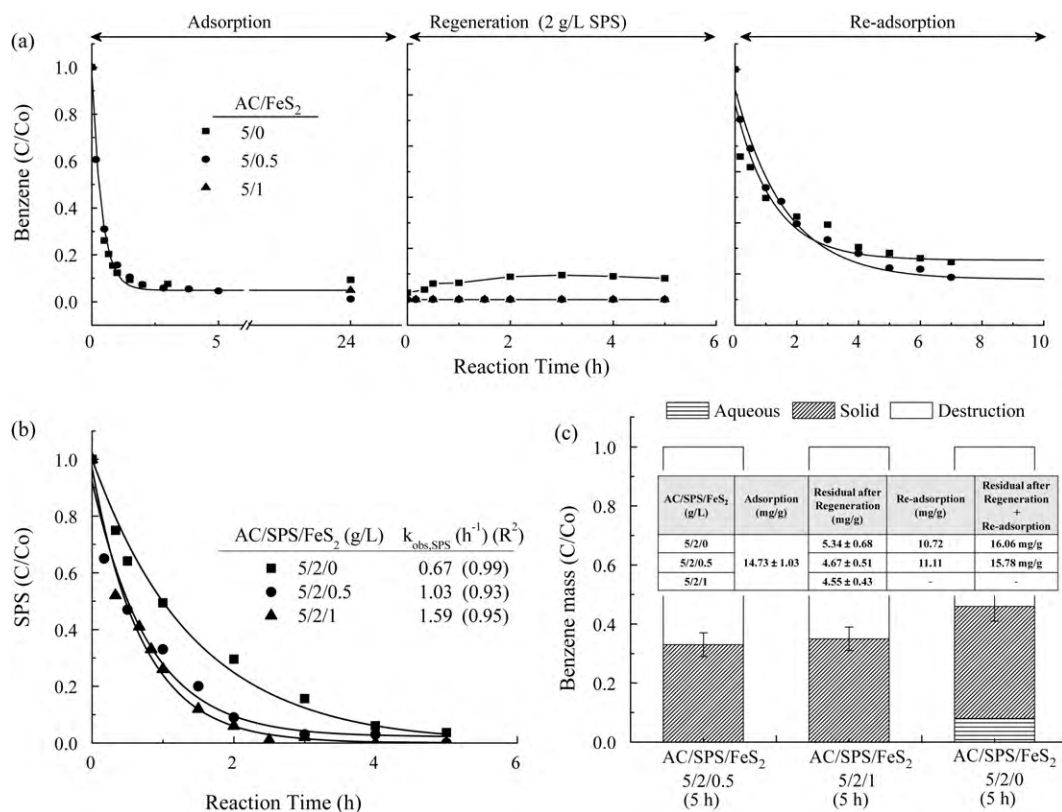


Fig. 5. Regeneration of benzene spent AC: (a) aqueous benzene variation; (b) persulfate regeneration; (c) mass balance among different phases after regeneration at 5 h.

sibly due to the occurrence of mild oxidation over the AC surfaces that were initially covered and saturated with benzene.

Kan and Huling [42] studied Fenton-driven regeneration of MTBE spent AC and indicated that MTBE oxidation is dependent on desorption and intra-particle diffusion. They also proposed that intra-particle diffusion is the limiting step for MTBE transport from AC to the aqueous phase. Therefore, the oxidation of sorbed contaminants could be constrained due to the short life-span of the radical oxidants such as sulfate radicals which originate mainly near the AC surface and hence are incapable of reaching to the deeper adsorption sites. Furthermore, the amount of AC sorbed benzene was not reduced when a higher pyrite concentration was used (i.e., from 0.5 to 1 g/L). The reason for this could be that excess Fe²⁺ released from pyrite in the system induced a faster persulfate degradation rate (i.e., 1.59 h⁻¹ in the presence of 1.0 g/L pyrite) and also scavenged SO₄^{-•} (i.e., SO₄^{-•} + Fe²⁺) [43]. Similar observations in the application of combining H₂O₂ and pyrite for oxidation of 2,4,6-trinitrotoluene were reported that increased pyrite did not enhance contaminant removal instead of slowing down the degradation reaction [21].

4. Conclusions

In this work, the interaction of activated carbon (AC) with persulfate anions has been investigated. The adsorption behaviors with AC or PS oxidized AC (OAC) have been characterized using pseudo-first-, -second-order kinetics, intra-particle diffusion models, and Freundlich and Langmuir isotherms. Persulfate oxidation of AC resulted in a loss of electrons on the AC and produced acidic functional groups, which led to a weakening of the AC dispersive interaction with benzene. Moreover, the changes in the chemical structure and characteristics of ACs are dependent on the direct contact of persulfate with the AC. For instance, when the adsorbent (i.e., benzene) was absent, the resulting oxidized AC

(i.e., OAC) showed a decrease in adsorptive capacity. The reduction in adsorption was mainly due to the hydration of the increased AC surface acidities and the presence of water clusters on the AC pores which resulted in a reduction in the surface area available for benzene adsorption. Experiments were carried out to investigate the effects of the simultaneous presence of persulfate and AC or persulfate/FeS₂ on benzene adsorption and degradation. The results show that the AC/SPS/FeS₂ system offers an effective method for destroying benzene that has been sorbed onto AC or, in the case of the AC/SPS system, desorbed in the aqueous phase. Furthermore, it was demonstrated that when SPS was used for regenerating benzene spent carbon, SPS oxidation resulted mainly in desorption of benzene from the AC. In contrast, no aqueous benzene was observed in the SPS/FeS₂ system, i.e., complete destruction of benzene in the aqueous phase was achieved. Despite this, the regenerated AC with the SPS or SPS/FeS₂ still retained its adsorptive capacity. On the basis of these findings, the oxidation systems put forward in this study may serve as a reference for potential on-site chemical oxidative regeneration of AC PRB application.

Acknowledgement

This study was partially funded by the National Science Council (NSC) of Taiwan under project number of NSC 98-2622-E-005-005-CC2.

Appendix A. Supplementary data

Supplementary data associated with this article can be found, in the online version, at doi:10.1016/j.jhazmat.2010.06.066.

References

- [1] ATSDR, Toxicological Profile for Benzene, Agency for Toxic Substances and Disease Registry (ATSDR), 2007. Available from: <<http://www.atsdr.cdc.gov/>>.
- [2] ATSDR, Benzene Toxicity, Agency for Toxic Substances and Disease Registry (ATSDR), 2001. Available from: <<http://www.atsdr.cdc.gov/>>.
- [3] B. Haist-Gulde, G. Baldauf, H.J. Brauch, Removal of organic micropollutants by activated carbon, in: J. Hrubeč (Ed.), *Water Pollution: Drinking Water and Drinking Water Treatment, Handbook of Environmental Chemistry*, Springer Verlag, New York, 1995.
- [4] D.J.D. Renzo, *Pollution Control Technology for Industrial Wastewater*, Noyes Data Corporation, Park Ridge, NJ, 1981.
- [5] L.R. Radovic, I.F. Silva, J.I. Ume, J.A. Menéndez, C.A. Leon, Y. Leon, A.W. Scaroni, An experimental and theoretical study of the adsorption of aromatics possessing electron-withdrawing and electron-donating functional groups by chemically modified activated carbons, *Carbon* 35 (1997) 1339–1348.
- [6] F. Villacañas, M.F.R. Pereira, J.J.M. Órfão, J.L. Figueiredo, Adsorption of simple aromatic compounds on activated carbons, *J. Colloid Interface Sci.* 293 (2006) 128–136.
- [7] F. Haghseresht, S. Nouri, J.J. Finnerty, G.Q. Lu, Effects of surface chemistry on aromatic compound adsorption from dilute aqueous solutions by activated carbon, *J. Phys. Chem. B* 106 (2002) 10935–10943.
- [8] T. Karanfil, S.A. Dastgheib, Trichloroethylene adsorption by fibrous and granular activated carbons: aqueous phase, gas phase, and water vapor adsorption studies, *Environ. Sci. Technol.* 38 (2004) 5834–5841.
- [9] N. Wibowo, L. Setyadhi, D. Wibowo, J. Setiawan, S. Ismadji, Adsorption of benzene and toluene from aqueous solutions onto activated carbon and its acid and heat treated forms: influence of surface chemistry on adsorption, *J. Hazard. Mater.* 146 (2007) 237–242.
- [10] USEPA, *Permeable Reactive Barrier Technologies for Contaminant Remediation*, United States Environmental Protection Agency (USEPA), 1998 (EPA/600/R-98/125).
- [11] D.W. Blowes, C.J. Ptacek, S.G. Benner, C.W.T. McRae, T.A. Bennett, R.W. Puls, Treatment of inorganic contaminants using permeable reactive barriers, *J. Contam. Hydrol.* 45 (2000) 123–137.
- [12] M.L. Crimi, J. Taylor, Experimental evaluation of catalyzed hydrogen peroxide and sodium persulfate for destruction of BTEX contaminants, *Soil Sediment Contam.* 16 (2007) 29–45.
- [13] C. Liang, C.-F. Huang, Y.-J. Chen, Potential for activated persulfate degradation of BTEX contamination, *Water Res.* 42 (2008) 4091–4100.
- [14] C. Liang, Y.-J. Chen, K.-J. Chang, Evaluation of persulfate oxidative wet scrubber for removing BTEX gases, *J. Hazard. Mater.* 164 (2009) 571–579.
- [15] D.A. House, Kinetics and mechanism of oxidations by peroxydisulfate, *Chem. Rev.* 62 (1962) 185–203.
- [16] V.L. Snoeyink, W.J. Weber Jr., The surface chemistry of active carbon: a discussion of structure and surface functional groups, *Environ. Sci. Technol.* 1 (1967) 228–233.
- [17] H.-H. Huang, M.-C. Lu, J.-N. Chen, C.-T. Lee, Catalytic decomposition of hydrogen peroxide and 4-chlorophenol in the presence of modified activated carbons, *Chemosphere* 51 (2003) 935–943.
- [18] A. Georgi, F.-D. Kopinke, Interaction of adsorption and catalytic reactions in water decontamination processes. Part I. Oxidation of organic contaminants with hydrogen peroxide catalyzed by activated carbon, *Appl. Catal. B: Environ.* 58 (2005) 9–18.
- [19] K. Okawa, K. Suzuki, T. Takeshita, K. Nakano, Regeneration of granular activated carbon with adsorbed trichloroethylene using wet peroxide oxidation, *Water Res.* 41 (2007) 1045–1051.
- [20] M. Kimura, I. Miyamoto, Discovery of the activated-carbon radical AC⁺ and the novel oxidation-reactions comprising the AC/AC⁺ cycle as a catalyst in an aqueous solution, *Bull. Chem. Soc. Jpn.* 67 (1994) 2357–2360.
- [21] M. Arienzo, Oxidizing 2,4,6-trinitrotoluene with pyrite–H₂O₂ suspensions, *Chemosphere* 39 (1999) 1629–1638.
- [22] R.D. Ludwig, D.J.A. Smyth, D.W. Blowes, L.E. Spink, R.T. Wilkin, D.G. Jewett, C.J. Weisener, Treatment of arsenic, heavy metals, and acidity using a mixed ZVI-compost PRB, *Environ. Sci. Technol.* 43 (2009) 1970–1976.
- [23] S. Cao, G. Chen, X. Hu, P.L. Yue, Catalytic wet air oxidation of wastewater containing ammonia and phenol over activated carbon supported Pt catalysts, *Catal. Today* 88 (2003) 37–47.
- [24] J.S. Noh, J.A. Schwarz, Effect of HNO₃ treatment on the surface acidity of activated carbons, *Carbon* 28 (1990) 675–682.
- [25] C. Liang, C.-F. Huang, N. Mohanty, R.M. Kurakalva, A rapid spectrophotometric determination of persulfate anion in ISCO, *Chemosphere* 73 (2008) 1540–1543.
- [26] F. Lucking, H. Koser, M. Jank, A. Ritter, Iron powder, graphite and activated carbon as catalysts for the oxidation of 4-chlorophenol with hydrogen peroxide in aqueous solution, *Water Res.* 32 (1998) 2607–2614.
- [27] B.K. Pradhan, N.K. Sandle, Effect of different oxidizing agent treatments on the surface properties of activated carbons, *Carbon* 37 (1999) 1323–1332.
- [28] I.I. Salame, T.J. Bandosz, Study of water adsorption on activated carbons with different degrees of surface oxidation, *J. Colloid Interface Sci.* 210 (1999) 367–374.
- [29] I.I. Salame, T.J. Bandosz, Role of surface chemistry in adsorption of phenol on activated carbons, *J. Colloid Interface Sci.* 264 (2003) 307–312.
- [30] L.B. Khalil, B.S. Giris, T.A. Tawfik, Decomposition of H₂O₂ on activated carbon obtained from olive stones, *J. Chem. Technol. Biotechnol.* 76 (2001) 1132–1140.
- [31] C. Liang, Y.-T. Lin, W.-H. Shin, Persulfate regeneration of trichloroethylene spent activated carbon, *J. Hazard. Mater.* 168 (2009) 187–192.
- [32] C. Liang, Y.-T. Lin, W.-H. Shih, Treatment of trichloroethylene by adsorption and persulfate oxidation in batch studies, *Ind. Eng. Chem. Res.* 48 (2009) 8373–8380.
- [33] I.A.W. Tan, B.H. Hameed, A.L. Ahmad, Equilibrium and kinetic studies on basic dye adsorption by oil palm fibre activated carbon, *Chem. Eng. J.* 127 (2007) 111–119.
- [34] Y.S. Ho, Review of second-order models for adsorption systems, *J. Hazard. Mater.* B136 (2006) 681–689.
- [35] Y.S. Ho, G. McKay, Pseudo-second order model for sorption processes, *Process Biochem.* 34 (1999) 451–465.
- [36] A.T. Mohd Din, B.H. Hameed, A.L. Ahmad, Batch adsorption of phenol onto physicochemical-activated coconut shell, *J. Hazard. Mater.* 161 (2009) 1522–1529.
- [37] C.H. Tessmer, R.D. Vidic, L.J. Uranowski, Impact of oxygen-containing surface functional groups on activated carbon adsorption of phenols, *Environ. Sci. Technol.* 31 (1997) 1872–1878.
- [38] P.M. Alvarez, F.J. Beltran, V. Gomez-Serrano, J. Jaramillo, E.M. Rodriguez, Comparison between thermal and ozone regenerations of spent activated carbon exhausted with phenol, *Water Res.* 38 (2004) 2155–2165.
- [39] R. Matta, K. Hanna, S. Chiron, Fenton-like oxidation of 2,4,6-trinitrotoluene using different iron minerals, *Sci. Total Environ.* 385 (2007) 242–251.
- [40] T.N. Das, Reactivity and role of SO₅^{•-} radical in aqueous medium chain oxidation of sulfite to sulfate and atmospheric sulfuric acid generation, *J. Phys. Chem. A* 105 (2001) 9142–9155.
- [41] P. Neta, V. Madhavan, H. Zemel, R.W. Fessenden, Rate constants and mechanism of reaction of SO₄^{•-} with aromatic compounds, *J. Am. Chem. Soc.* 99 (1977) 163–164.
- [42] E. Kan, S.G. Huling, Effects of temperature and acidic pre-treatment on Fenton-driven oxidation of MTBE-spent granular activated carbon, *Environ. Sci. Technol.* 43 (2009) 1493–1499.
- [43] C. Liang, C.J. Bruell, M.C. Marley, K.L. Sperry, Persulfate oxidation for in situ remediation of TCE. I. Activated by ferrous ion with and without a persulfate–thiosulfate redox couple, *Chemosphere* 55 (2004) 1213–1223.